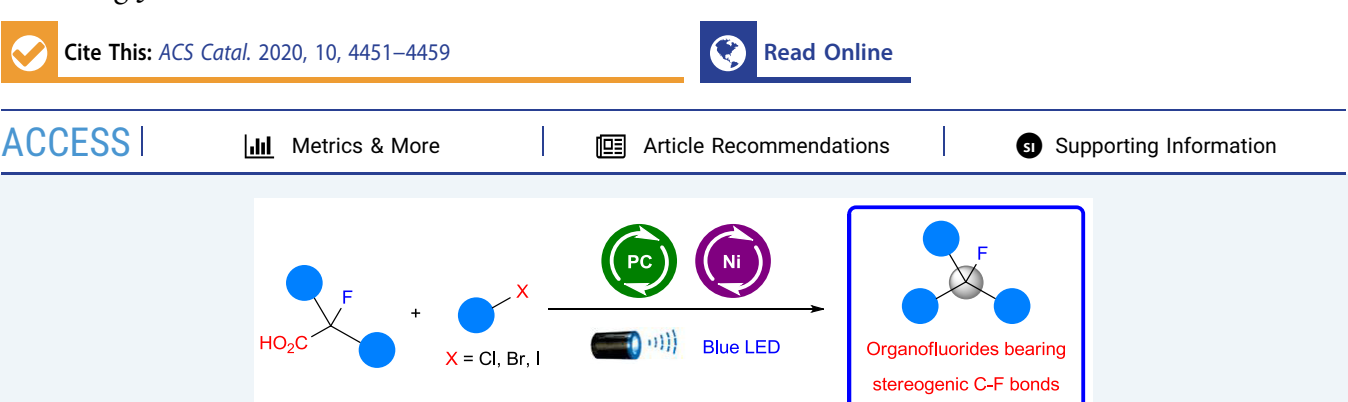


pubs.acs.org/acscatalysis Letter

Engaging α -Fluorocarboxylic Acids Directly in Decarboxylative C–C Bond Formation

Hongyu Wang, Chen-Fei Liu, Zhihui Song, Mingbin Yuan, Yee Ann Ho, Osvaldo Gutierrez, and Ming Joo Koh*



ABSTRACT: Fluorine-containing organic molecules, particularly those that bear (sp^3) C–F bonds, are rapidly gaining prominence in modern chemical synthesis. Although extensive studies have been devoted to the preparation of secondary and tertiary fluorides, crucial shortcomings remain: for example, lengthy substrate synthesis, contrived installation of difficult-to-remove directing/activating units, excessive waste generation and/or limited functional group compatibility. Here, we show that readily accessible α-monofluoro carboxylic acids, which are conventionally difficult substrates for cross-coupling, undergo direct decarboxylative cross-coupling with sp^2 - and sp^3 -hybridized organohalides to afford a wide assortment of fluorinated products. Reactions are typically promoted by a combination of 1 mol % of an Ir-based photocatalyst and 2–15 mol % of a bipyridine–Ni complex, delivering products in up to 86% yield under blue LED light irradiation. Concise synthesis of key therapeutic candidates underscores utility, complementarity, and distinct advantages compared with existing methods. DFT calculations are used to rationalize the distinct reactivity of α-fluoro carboxylic acid substrates (vs nonfluorinated parent acids) under decarboxylation conditions.

KEYWORDS: fluorine, carboxylic acids, cross-coupling, decarboxylation, metallaphotoredox, dual catalysis

he strategic replacement of a C-H bond of an organic molecule with a C-F unit can often impart desirable properties, an effect that largely arises from the significant polarization of electron density toward the electronegative fluorine atom. Over the last few decades, chemists have capitalized on this strategy to access rationally designed organofluorine compounds that bear stereogenic C-F centers,² contributing profoundly to the discovery of new therapeutic agents,³ agrochemicals,⁴ and materials.⁵ The utility of organofluorides extends beyond enhancing the properties of a biologically active molecule or functional material. Owing to repulsive electronic interactions and the fluorine gauche effect⁶ $(\sigma_{C-H} \to \sigma^*_{C-F})$ hyperconjugation, C-F entities may induce conformational rigidity within the carbon skeleton; this has been exploited to promote enantioselectivite processes, to determine the active conformation(s) and mode of action of drug molecules⁸ as well as to develop new catalysts.⁹

A prominent set of monofluorinated compounds that commonly reside within pharmaceutically important scaffolds are those that contain (sp³)C-F bonds (Scheme 1a). Protocols that deliver secondary and tertiary alkyl fluorides have been reported. Directed or undirected fluorination of aliphatic C-H bonds, 10 either involving a metal-based

catalyst¹¹ or through photocatalytic¹² or electrochemical pathways,¹³ provides a direct entry to secondary and tertiary fluorides, although chemo- and site selectivity can be challenging in the presence of other similarly reactive functional groups and/or C–H bonds. Another common strategy to access organofluorides pertains to substitution reactions involving carboxylic acids,¹⁴ alcohols,¹⁵ or their derivatives¹⁶ in the presence of a nucleophilic or electrophilic fluorinating reagent. These transformations are sometimes plagued by undesired elimination side reactions which can lead to complex mixtures and diminished yields. Hydro- and carbofluorination of alkenes and allenes¹⁷ provide an alternative option to access fluoroalkanes, although the scope is restricted to certain π systems due to regioselectivity complications. An attractive approach to aliphatic mono-

Received: February 15, 2020 Revised: March 23, 2020 Published: March 24, 2020



Scheme 1. Significance of Organofluorides Bearing Stereogenic C-F Bonds and Catalytic Cross-Coupling Strategies to Access Them

fluorides that offers a convenient platform to generate molecular complexity from simpler substrates involves the union of a nucleophilic organometallic species (e.g., zinc- or boron-based reagents)¹⁸ or an organohalide¹⁹ with fluorinated electrophiles to facilitate chemoselective C–C bond formation through catalytic cross-coupling or Heck-type reactions.²⁰

Comm. available or readily accessible
Carboxyl unit as activating group for

Straightforward

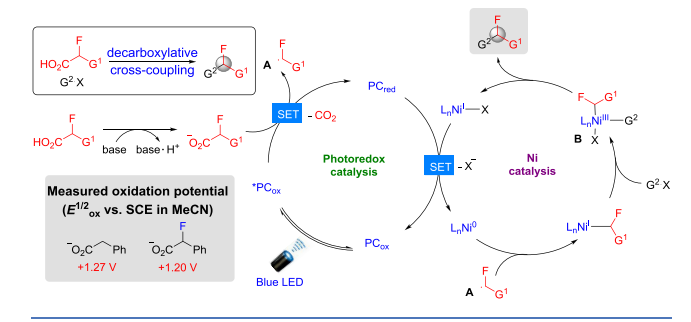
Stable, abundant

However, state-of-the-art advances in catalytic crosscoupling suffer from a number of critical shortcomings 18,19 (Scheme 1b): (a) laborious multistep synthesis of the fluorinated electrophile, (b) excessive waste generation, and/ or (c) limited functional group compatibility (e.g., reactions that afford sterically encumbered tertiary fluorides are scarce, and reported cases require high catalyst loadings). An efficient catalytic cross-coupling protocol that enables a readily accessible fluorine-containing cross-partner to be utilized in conjunction with a second reagent would be complementary to existing protocols and particularly advantageous in enhancing the way with which many high-value organofluorine building blocks are currently prepared. In light of this deliberation, we sought to devise a new strategy that leverages α -fluorocarboxylic acids as substrates; these compounds are either commercial or easily derived from abundant, stable, and readily available feedstock chemicals such as amino acids, 21 carboxylic acids, 22 and esters 23 by nucleophilic substitution or α-fluorination of the in situ-generated enolate/enol ether intermediates (Scheme 1c, inset). Through photoredox decarboxylative cross-coupling with an appropriate organohalide 9 (stable and easily accessible), we envision transforming racemic α -fluoro acids 10 directly to a myriad of functionalized secondary and tertiary fluorides 1 with concomitant extrusion of CO₂ (Scheme 1c).

In designing reactions that furnish fluoroalkanes, we wondered if metallaphotoredox-catalyzed cross-coupling may be exploited to promote formation of the desired fluorinated products.²⁴ As illustrated in the proposed catalytic pathway

(Scheme 2), our initial concerns were: (i) whether the α -fluoro acid can undergo efficient single electron transfer (SET) to

Scheme 2. Proposed Pathway to Access Organofluorides by Metallaphotoredox Decarboxylative Cross-Coupling



afford the putative α -fluoroalkyl radical species **A** and its associated lifetime; (ii) how efficient does **A** engage with the nickel-based complex to turn over the catalytic cycle. Adding to the uncertainty is a recent study suggesting that α -fluoro acids are *reluctant* to undergo decarboxylative C–C bond formation. ²⁵

Cyclic voltammetry experiments (Scheme 2, gray box) revealed that the oxidation potentials of 2-phenylacetate and its α -fluoro variant (in the form of tetrabutylammonium salts) were similar (see Supporting Information for details), implying that these carboxylates should undergo SET in the presence of a suitable photocatalyst and irradiation to give the corresponding radical intermediates with similar ease. The challenge remains whether **A** is sufficiently long-lived to participate in the Ni-catalyzed cross-coupling cycle and deliver the desired product after reaction with the organohalide cross-partner.

As shown in Scheme 3, under previously established conditions for photoredox decarboxylation in the presence of

Scheme 3. Deleterious Effect of Fluorine in Metallaphotoredox Decarboxylative Cross-Coupling of Carboxylic Acids

1 mol % of **Ir-1a** and 2 mol % of a Ni-based catalyst, ^{24a,b} phenylacetic acid **10a**′ undergoes efficient decarboxylative cross-coupling with aryl bromide **9a** to deliver **1a**′ in 90% yield. Unfortunately, the desired analogous conversion of 2-fluoro-2-phenylacetic acid **10a** to fluorinated compound **1a** was in efficient (25% conv., 15% yield).

To gain some insight into disparate reactivity profiles observed, we performed a series of unrestricted, dispersion-corrected density functional theory (DFT) computations using implicit solvent (Figure 1). On the basis of our prior work, we deemed it was necessary to consider various spin states (singlet/triplet and doublet/quartet), potential pathways including Ni(0)/Ni(II)/Ni(III) and Ni(0)/Ni(1)/Ni(III), and inner-sphere and outer-sphere C–C bond formation. For simplicity, only the lowest-energy pathway is shown and will be discussed in the text (see Supporting Information for full energy diagrams).

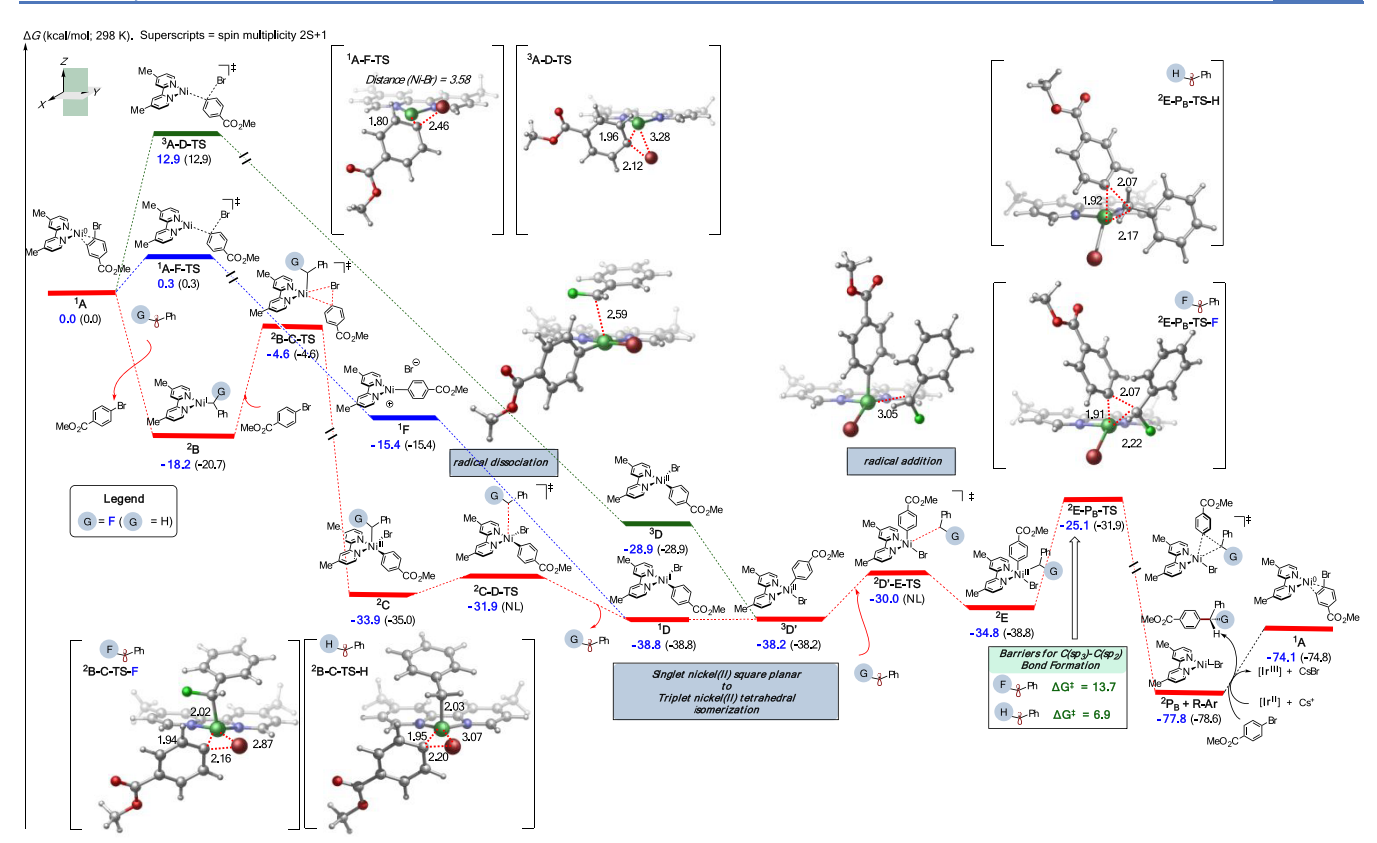


Figure 1. Comparison between lowest energy Ni-catalyzed cross-coupling between fluorinated benzyl radical (blue) and unsubstituted benzyl radical (in parentheses). All free energies (kcal/mol) were determined at the UB3LYP-D3/def2-TZVPP-CPCM(DMA)//UB3LYP-D3/def2-SVP-CPCM(DMA) level of theory.

As shown in Figure 1, assuming presence of the benzyl radicals in solution, presumably formed from SET with photocatalyst and concomitant CO₂ release (Scheme 2),²⁴ we found a barrierless addition to Ni(0) to form a Ni(I)-benzyl intermediate (2B), downhill by 18.2 and 20.7 kcal/mol for fluorinated (G = F) and unsubstituted (G = H) radical, respectively. In turn, this intermediate is poised to undergo facile oxidative addition (via doublet spin state ²B-C-TS) to form the corresponding Ni(III) intermediate ²C. Closer inspection at the lowest-energy oxidative addition transition states (2B-C-TS-F and 2B-C-TS-H) reveals an earlier transition state for the unsubstituted system as evident by the bond breaking/forming distances in comparison to the fluorinated benzyl radical. At this stage the exergonicities (from Ni(0) and corresponding radical) for both fluorinated- and unsubstituted benzyl radical, G = F and H, respectively, are nearly identical (i.e., downhill in energy by ca. 34-35 kcal/ mol). Notably, direct C-C bond formation from Ni(III) ²C (e.g., inner sphere reductive elimination) could not be located. Instead, in agreement with previous calculations,^{27d} this Ni(III) ²C intermediate, with C(sp³) moiety along the z-axis, is poised to undergo nearly barrierless radical dissociation (i.e., relative barrier is only 2 kcal/mol via 2C-D-TS) to form the square planar Ni(II) intermediate ¹D, downhill in energy by ~5 kcal/mol.²⁸ Further, to undergo effective inner-sphere C-C bond formation, this Ni(II) intermediate must undergo an isomerization-intersystem crossing to form the tetrahedral Ni(II) intermediate ³D', which is nearly isoenergetic to the square planar Ni(II). Finally, facile radical addition (via ²D'-E-TS) to the tetrahedral Ni(II) intermediate ³D' will form the productive Ni(III) ${}^{2}E$ with $C(sp^{2})$ moiety along the z-axis that is

poised to undergo *inner-sphere* reductive elimination (via 2E - P_B -TS) leading to the desired cross-coupled product and Ni(I). Finally, subsequent SET from the reduced form of photocatalyst could regenerate the Ni(0) catalytic species 1A and restart the nickel radical cross-coupling cycle, with concomitant formation of CsBr complex. 29

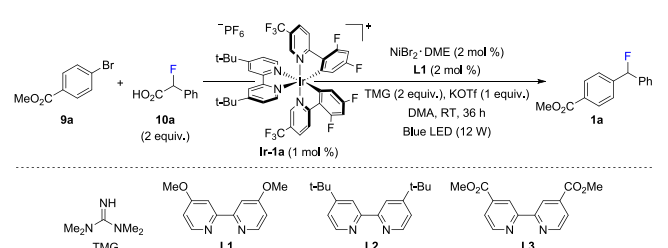
Alternatively, if the radical concentration is low, the Ni(0)¹A could instead engage with the aryl bromide to do an nearly barrierless S_NAr-type addition (barrier only 0.3 kcal/mol via ¹A-F-TS) leading to ¹F'···Br complex, which can rearrange to give the square planar Ni(II) intermediate ¹D. Notably, we found that the commonly proposed direct and concerted oxidative addition from Ni(0) to Ni(II) (i.e., ³A-F-TS) is much higher in energy and proceeds via the triplet spin state. These results underscore the need to consider various spin states, include dispersion corrections, and solvent effects in the optimizations because these can change the nature of the mechanism in nickel radical cross-couplings. Finally, the persistent nickel(II) intermediate ¹D can then engage with the transient benzylic radical, presumably from generation from the photocatalytic cycle,²⁴ to undergo inner-sphere C–C bond formation. Overall, a direct comparison of the lowest energy pathways between fluoro-substituted (blue) and unsubstituted benzyl system (in parentheses) revealed similar mechanistic pictures (see Figure S1 and Figure S2 in Supporting Information). However, for the unsubstituted system $(\tilde{G} = H)$, the Ni(III)-Ni(II)-Ni(III) isomerization energy surface is flatter. For example, despite numerous attempts, the radical addition to the square planar or tetrahedral Ni(II) intermediates (i.e., ²C-D-TS and ²D'-E-

TS) could not be located and is likely barrierless. Importantly, we observe a much larger relative barrier for the $C(sp^2)$ -C(sp³) bond formation (from Ni(II)) for the fluorosubstituted benzyl radical (13.7 kcal/mol) than for the unsubstituted system (6.9 kcal/mol). Presumably the higher barrier is due to greater electrostatic repulsion between the C-F and Ni-Br bonds in the reductive elimination transition state (²E-P_B-TS) that is absent in the unsubstituted system.³⁰ We hypothesize that the computed higher barrier for innersphere $C(sp^2)-C(sp^3)$ bond formation could contribute to the lower efficiency observed for the fluorinated systems and could open further opportunities for undesired side reactions such as hydrogen atom abstraction (e.g., with solvent molecules).31 Given (1) the nearly identical redox potentials for fluorinated and nonfluorinated radical precursors (Scheme 2, inset), and (2) lower reactivity for fluorinated systems under identical conditions and catalytic system (Scheme 3), we favor the stepwise oxidative addition (via S_NAr mechanism) Ni(0)/ Ni(II) pathway followed by rate-limiting $C(sp^2)-C(sp^3)$ bond formation. As such, we attribute the distinct reactivity to relative barriers for inner-sphere C(sp²)-C(sp³) which are significantly higher for the fluorinated benzylic radicals (G = F)than unsubstituted benzyl system (13.7 vs 6.9 kcal/mol). Notably, in both cases the barriers for SET transfer step to regenerate the catalytic Ni(0) species should be identical. Taken together, these results highlight that α -fluorocarboxylic acids are inherently more challenging substrates for crosscoupling.

Given that barriers for $C(sp^2)-C(sp^3)$ bond formation with fluoro-substituted benzyl radicals are not insurmountable (~14 kcal/mol; Figure 1), we hypothesize that further reaction optimization could to be devised in order to achieve the desired decarboxylative cross-coupling of α -fluoro acids. The reaction of 9a and 10a to afford 1a was used as the model reaction for optimization studies (Table 1). Gratifyingly, after an extensive survey of various photocatalysts, nickel salts, ligands, bases, additives, and solvents (see Supporting Information for further details), we found that la can be generated in 86% yield in the presence of 1 mol % of Ir-1a, 2 mol % of a Ni-based complex derived from NiBr2·DME and dimethoxy-substituted L1, 1,1,3,3-tetramethylguanidine (TMG) as the base and stoichiometric potassium triflate (KOTf) additive in DMA at ambient temperature under blue LED irradiation (entry 1). As expected, no product was detected in the absence of blue light or any of the required catalysts (entry 2). Diminished product yields were obtained when other Ni salts (entries 3 and 4) or more electrondeficient bipyridine ligands L2 and L3 (entries 5 and 6) were

Switching the solvent from DMA to other variants such as DMF NMP, DMPU, DMSO or toluene also lowered efficiency (entries 7–11), suggesting that a reasonably polar medium is necessary to stabilize the intermediate radical and/or organometallic species without affecting their ability to undergo reaction. What is more, with NMP and DMPU, significant amounts of byproducts (\sim 30–40%) arising from reaction of solvent molecules with 9a could be detected. Keeping all other parameters constant, conducting the cross-coupling in the absence of KOTf resulted in an appreciable drop in efficiency (entry 12). Although it remains to be determined, we reasoned that the triflate anion may play a role in ligand substitution to form a more activated Ni-based complex **B** (X = Br \rightarrow X = OTf; see Scheme 2), consequently reducing the

Table 1. Evaluation of Reaction Conditions^a



entry	deviation from standard conditions	yield (%) ^a
1	none	86
2	no photocatalyst, no nickel catalyst, or no light	<2
3	NiCl ₂ ·DME instead of NiBr ₂ ·DME	70
4	Ni(COD) ₂ instead of NiBr ₂ ·DME	75
5	L2 instead of L1	45
6	L3 instead of L1	38
7	DMF instead of DMA	76
8	NMP instead of DMA	50
9	DMPU instead of DMA	65
10	DMSO instead of DMA	30
11	toluene instead of DMA	trace
12	No KOTf	76
13	NaOTf instead of KOTf	65
14	LiOTf instead of KOTf	73
15	DBU instead of TMG	75
16	Cs ₂ CO ₃ instead of TMG	50
17	K ₂ CO ₃ instead of TMG	55
18	KOt-Bu instead of TMG	trace

"The reaction was carried out with 9a (0.1 mmol), 10a (0.2 mmol), NiBr₂.DME (2 mol %), L1 (2 mol %), TMG (0.2 mmol), KOTf (0.1 mmol), and Ir-1a (1 mol %) in DMA under blue LED. DME, 1,2-dimethoxyethane; DMA, N,N-dimethylacetamide; DMF, N, N-dimethylformamide; NMP, N-methyl-2-pyrrolidone; DMPU, N,N'-dimethylpropyleneurea; DMSO, dimethyl sulfoxide; DBU, 1,8-diazabicyclo[5.4.0]undec-7-ene; COD, 1,5-cyclooctadiene; RT, room temperature. Yields are for isolated and purified products.

barrier to facilitate reductive elimination.³⁴ The triflate additive might also suppress formation of any inactive Ni-F species.³⁵ Replacing KOTf with other triflate additives, however, gave poorer results (entries 13 and 14). Finally, the effect of the external base was probed. For reasons that are unclear at this moment, it was discovered that the more basic organic variants (e.g., TMG and DBU in entries 1 and 15) led to better conversions to 1a and minimal byproduct formation from reaction of 9a with DMA (vs less basic inorganic carbonate bases (\sim 20-30% byproduct) in entries 16 and 17). Use of a stronger alkoxide base was considerably less efficient (entry 18), owing to decomposition of 10a and other competing side reactions. Further mechanistic experiments, from theory and experiment, are ongoing to elucidate the role of KOTf, base, and the mechanism, likely very different than that discussed earlier, in this new catalytic system and will be reported in due

With the established conditions in hand, we next assessed the generality of our protocol with a range of functionalized α -fluorocarboxylic acids (1b-q, Scheme 4). In general, 2-fluoro-2-arylacetic acids bearing *ortho-, meta-,* or *para-substituents* on the aryl ring served as effective substrates, furnishing the desired secondary fluorides 1b-k in 40–76% yield. Reactions with 2-fluoro-2-alkylacetic acids proceeded to give the products 1l-n, although yields were slightly diminished

Scheme 4. Secondary and Tertiary fluorides Accessible by Photoredox Decarboxylative Cross-Coupling^a

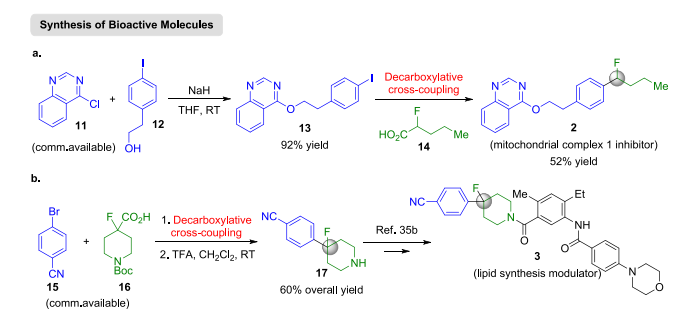
"Unless otherwise stated, all reactions were conducted using bromides 9 (X = Br) under the optimized conditions. Yields are for isolated and purified products. For the synthesis of 11–n, reactions were conducted using 10 mol % of NiBr2·DME and 12 mol % of L1. For the synthesis of 10–q and 1af–ai, reactions were conducted using 15 mol % of NiCl2·DME and 20 mol % of L2 in the absence of KOTf. For the synthesis of 1r–t, reactions were conducted using iodides 9 (X = I) in the absence of KOTf. For the synthesis of 1am–aq, reactions were conducted using chlorides 9 (X = Cl) in the absence of KOTf.

presumably because of the comparatively lower stability of the intermediate α -fluoroalkyl radical involved (see A, G^1 = alkyl vs G^1 = aryl, Scheme 2). Notably, the present catalytic protocol can be extended to sterically demanding tertiary fluorides $(\mathbf{1o-q})$ using 15 mol % of a Ni-based catalyst, which is more practical than previous cross-coupling methods employing more difficult-to-access fluorinated substrates and higher catalyst loadings. Additionally, synthesis of $\mathbf{1o-q}$ by alternative procedures involving aryllithium addition to the corresponding ketone followed by deoxyfluorination is impractical owing to poor yields and susceptibility of the ester moiety toward strong organometallic nucleophiles.

In addition to varying the α -fluoro acid cross-partner, we also examined a wide assortment of aryl and heteroaryl halides (1r-al, Scheme 4). Under our standard conditions, the corresponding secondary or tertiary fluorides can be obtained in 43–77% yield. These include products that contain a cyanide (1u), an aldehyde (1v, 1w, 1ag), a ketone (1x, 1af), an ester (1aj, 1al), a lactone (1y), an amide (1ak), an acetal (1aj, 1ak) as well as heterocyclic units (1z, 1aa-ae, 1ah, 1ai). Besides sp²-hybridized carbon electrophiles, the method is also amenable to sp³-hybridized organohalides, delivering alkyl fluorides 1am-aq in 50–60% yield albeit as inseparable diastereomeric mixtures.

The first application that showcases utility of our protocol relates to the preparation of MMP-mitochondrial complex 1 inhibitor 2, which was discovered to be more potent than its nonfluorinated derivative³⁷ (Scheme 5a). Etherification of 11

Scheme 5. Application to Concise Synthesis of Fluorinated Bioactive $Molecules^a$



"All catalytic decarboxylative reactions were conducted under the optimized conditions from Scheme 4. Yields are for isolated and purified products. See Supporting Information for details.

with 12 (both commercially available) afforded iodide 13, which was subjected to photoredox decarboxylative cross-coupling with α -fluoro acid 14 (synthesized from valeric acid) to furnish the desired secondary fluoride 2 in 47% overall yield over two steps. It merits mention that the alternative benzylic C–H fluorination³⁸ route to access 2 could pose regioselectivity complications (two benzylic sites available), whereas synthesis of 2 through alcohol formation followed by deoxyfluorination³⁹ is less convergent.

In another instance (Scheme 5b), the catalytic union of bromide 15 with α -fluoro acid 16 (both commercially available) followed by Boc deprotection conveniently generated tertiary fluoride 17, an intermediate used to access lipid synthesis modulator 3, in 60% overall yield. The present two-step formal synthesis is more concise than a previous procedure in which 17 was obtained in four steps with 22% overall yield. Both applications highlight the distinct

advantages of decarboxylative transformations for the efficient synthesis of functionalized monofluorinated compounds under mild reaction conditions.

The synthesis of secondary and tertiary fluorides was successfully accomplished by merging stable and readily accessible α -fluorocarboxylic acids with organohalides through catalytic photoredox decarboxylation. Contrary to nonfluorinated carboxylic acids, the corresponding α -fluoro analogues were found to be much less effective for decarboxylative crosscoupling. These observations were rationalized by the inherently higher barrier for C-C bond formation with α fluoroalkyl radicals as supported by DFT calculations. Development of new reaction conditions enabled α -fluoro acids to serve as effective substrates for cross-coupling, providing access to a diverse range of functionalized organofluorine building blocks and pharmaceuticals. The method is expected to advance fluorochemical synthesis, unravel new avenues toward the design of novel fluorine-containing drug candidates and aid efforts toward the development of new cross-coupling transformations involving fluorine-containing radical species. Ongoing mechanistic studies are geared toward understanding the mechanism of this system including elucidating the role of KOTf and TMG.

ASSOCIATED CONTENT

Supporting Information

The Supporting Information is available free of charge at https://pubs.acs.org/doi/10.1021/acscatal.0c00789.

Detailed experimental procedures, spectral data, and analytical data (PDF)

AUTHOR INFORMATION

Corresponding Authors

Ming Joo Koh — Department of Chemistry, National University of Singapore, Republic of Singapore 117549; orcid.org/0000-0002-2534-4921; Email: chmkmj@nus.edu.sg

Osvaldo Gutierrez — Department of Chemistry and Biochemistry, University of Maryland, College Park, Maryland 20742, United States; Occid.org/0000-0001-8151-7519; Email: ogs@umd.edu

Authors

Hongyu Wang – Department of Chemistry, National University of Singapore, Republic of Singapore 117549

Chen-Fei Liu — Department of Chemistry, National University of Singapore, Republic of Singapore 117549

Zhihui Song – Department of Chemistry and Biochemistry, University of Maryland, College Park, Maryland 20742, United States

Mingbin Yuan – Department of Chemistry and Biochemistry, University of Maryland, College Park, Maryland 20742, United States

Yee Ann Ho — Department of Chemistry, National University of Singapore, Republic of Singapore 117549; orcid.org/0000-0002-9886-8021

Complete contact information is available at: https://pubs.acs.org/10.1021/acscatal.0c00789

Author Contributions

§(H.W., C.-F.L.) These authors contributed equally.

Author Contributions

*(Z.S., M.Y.) These authors contributed equally.

Notes

The authors declare no competing financial interest.

ACKNOWLEDGMENTS

This research was supported by the National University of Singapore President's Assistant Professorship start-up grant (R-143-000-A50-133 to M.J.K.) and by the NSF (CAREER 1751568 to O.G.). O.G. is grateful to the University of Maryland College Park for start-up funds and computational resources from UMD Deepthought2 and MARCC/BlueCrab HPC clusters and XSEDE (CHE160082 and CHE160053).

REFERENCES

- (1) (a) O'Hagan, D. Understanding organofluorine chemistry. An introduction to the C-F bond. *Chem. Soc. Rev.* **2008**, *37*, 308–319. (b) Wang, J.; Sánchez-Roselló, M.; Aceña, J. L.; del Pozo, C.; Sorochinsky, A. E.; Fustero, S.; Soloshonok, V. A.; Liu, H. Fluorine in pharmaceutical industry: fluorine-containing drugs introduced to the market in the last decades (2001–2011). *Chem. Rev.* **2014**, *114*, 2432–2506
- (2) (a) Champagne, P. A.; Desroches, J.; Hamel, J.-D.; Vandamme, M.; Paquin, J.-F. Monofluorination of organic compounds: 10 years of innovation. *Chem. Rev.* **2015**, *115*, 9073–9174. (b) Zhu, Y.; Han, J.; Wang, J.; Shibata, N.; Sodeoka, M.; Soloshonok, V. A.; Coelho, J. A. S.; Toste, F. D. Modern approaches for asymmetric construction of carbon-fluorine quaternary stereogenic centers: synthetic challenges and pharmaceutical needs. *Chem. Rev.* **2018**, *118*, 3887–3964.
- (3) (a) Zhou, Y.; Wang, J.; Gu, Z.; Wang, S.; Zhu, W.; Aceña, J. L.; Soloshonok, V. A.; Izawa, K.; Liu, H. Next generation of fluorine-containing pharmaceuticals, compounds currently in phase II-III clinical trials of major pharmaceutical companies: new structural trends and therapeutic areas. *Chem. Rev.* 2016, 116, 422–518. (b) Gillis, E. P.; Eastman, K. J.; Hill, M. D.; Donnelly, D. J.; Meanwell, N. A. Applications of fluorine in medicinal chemistry. *J. Med. Chem.* 2015, 58, 8315–8359.
- (4) Fujiwara, T.; O'Hagan, D. Successful fluorine-containing herbicide agrochemicals. *J. Fluorine Chem.* **2014**, *167*, 16–29.
- (5) Berger, R.; Resnati, G.; Metrangolo, P.; Weber, E.; Hulliger, J. Organic fluorine compounds: a great opportunity for enhanced materials properties. *Chem. Soc. Rev.* **2011**, *40*, 3496–3508.
- (6) (a) Briggs, C. R. S.; Allen, M. J.; O'Hagan, D.; Tozer, D. J.; Slawin, A. M. Z.; Goeta, A. E.; Howard, J. A. K. The observation of a large gauche preference when 2-fluoroethylamine and 2-fluoroethanol become protonated. *Org. Biomol. Chem.* **2004**, *2*, 732–740. (b) Thacker, J. C. R.; Popelier, P. L. A. Fluorine gauche effect explained by electrostatic polarization instead of hyperconjugation: an interacting quantum atoms (IQA) and relative energy gradient (REG) study. *J. Phys. Chem. A* **2018**, *122*, 1439–1450. (c) Bentler, P.; Bergander, K.; Daniliuc, C. G.; Mück-Lichtenfeld, C.; Jumde, R. P.; Hirsch, A. K. H.; Gilmour, R. Inverting small molecule-protein recognition by the fluorine gauche effect: selectivity regulated by multiple H-F bioisosterism. *Angew. Chem., Int. Ed.* **2019**, *58*, 10990–10994.
- (7) (a) Cahard, D.; Bizet, V. The influence of fluorine in asymmetric catalysis. *Chem. Soc. Rev.* **2014**, *43*, 135–147. (b) Lee, K. A.; Silverio, D. L.; Torker, S.; Robbins, D. W.; Haeffner, F.; van der Mei, F. W.; Hoveyda, A. Catalytic enantioselective addition of organoboron reagents to fluoroketones controlled by electrostatic interactions. *Nat. Chem.* **2016**, *8*, 768–777.
- (8) Hunter, L. The C-F bond as a conformational tool in organic and biological chemistry. *Beilstein J. Org. Chem.* **2010**, *6*, 38.
- (9) (a) Sparr, C.; Gilmour, R. Fluoro-organocatalysts: conformer equivalents as a tool for mechanistic studies. *Angew. Chem., Int. Ed.* **2010**, 49, 6520–6523. (b) Zimmer, L. E.; Sparr, C.; Gilmour, R. Fluorine conformational effects in organocatalysis: an emerging strategy for molecular design. *Angew. Chem., Int. Ed.* **2011**, 50, 11860–11871. (c) Molnár, I. G.; Holland, M.C.; Daniliuc, C.; Houk, K.N.; Gilmour, R. Organocatalysis intermediates as platforms to study

noncovalent interactions: integrating fluorine gauche effects in iminium systems to facilitate acyclic conformational control. *Synlett* **2016**, *27*, 1051–1055.

- (10) (a) Lin, A.; Huehls, C. B.; Yang, J. Recent advances in C-H fluorination. *Org. Chem. Front.* **2014**, *1*, 434–438. (b) Ma, J.-A.; Li, S. Catalytic fluorination of unactivated C(sp³)-H bonds. *Org. Chem. Front.* **2014**, *1*, 712–715. (c) Szpera, R.; Moseley, D. F. J.; Smith, L. B.; Sterling, A. J.; Gouverneur, V. The fluorination of C-H bonds: developments and perspectives. *Angew. Chem., Int. Ed.* **2019**, *58*, 14824–14848.
- (11) (a) Bloom, S.; Pitts, C. R.; Woltornist, R.; Griswold, A.; Holl, M. G.; Lectka, T. Iron(II)-catalyzed benzylic fluorination. *Org. Lett.* **2013**, *15*, 1722–1724. (b) Xu, P.; Guo, S.; Wang, L.; Tang, P. Silver-catalyzed oxidative activation of benzylic C-H bonds for the synthesis of difluoromethylated arenes. *Angew. Chem., Int. Ed.* **2014**, *53*, 5955–5958. (c) Liu, W.; Huang, X.; Cheng, M.-J.; Nielsen, R. J.; Goddard, W. A.; Groves, J. T. Oxidative aliphatic C-H fluorination with fluoride ion catalyzed by a manganese porphyrin. *Science* **2012**, *337*, 1322–1325. (d) Braun, M.-G.; Doyle, A. G. Palladium-catalyzed allylic C-H fluorination. *J. Am. Chem. Soc.* **2013**, *135*, 12990–12993.
- (12) (a) Xia, J.-B.; Zhu, C.; Chen, C. Visible light-promoted metalfree C-H activation: diarylketone-catalyzed selective benzylic monoand difluorination. *J. Am. Chem. Soc.* **2013**, *135*, 17494–17500. (b) Bume, D. D.; Pitts, C. R.; Ghorbani, F.; Harry, S. A.; Capilato, J. N.; Siegler, M. A.; Lectka, T. Ketones as directing groups in photocatalytic sp³ C-H fluorination. *Chem. Sci.* **2017**, *8*, 6918–6923. (c) Nodwell, M. B.; Yang, H.; Čolović, M.; Yuan, Z.; Merkens, H.; Martin, R. E.; Bénard, F.; Schaffer, P.; Britton, R. ¹⁸F-fluorination of unactivated C-H bonds in branched aliphatic amino acids: direct synthesis of oncological positron emission tomography imaging agents. *J. Am. Chem. Soc.* **2017**, *139*, 3595–3598. (d) Danahy, K. E.; Cooper, J. C.; Van Humbeck, J. F. Benzylic fluorination of azaheterocycles induced by single-electron transfer to selectfluor. *Angew. Chem., Int. Ed.* **2018**, *57*, 5134–5138.
- (13) (a) Kuribayashi, S.; Kurioka, T.; Inagi, S.; Lu, H.-J.; Uang, B.-J.; Fuchigami, T. The selective electrochemical fluorination of S-alkyl benzothioate and its derivatives. *Beilstein J. Org. Chem.* **2018**, *14*, 389–396. (b) Takahira, Y.; Chen, M.; Kawamata, Y.; Mykhailiuk, P.; Nakamura, H.; Peters, B. K.; Reisberg, S. H.; Li, C.; Chen, L.; Hoshikawa, T.; Shibuguchi, T.; Baran, P. S. Electrochemical C(sp³)-H fluorination. *Synlett* **2019**, *30*, 1178–1182. (c) Cheng, Q.; Ritter, T. New diections in C-H fluorination. *Trends in Chem.* **2019**, *1*, 461–470
- (14) (a) Ventre, S.; Petronijevic, F. R.; MacMillan, D. W. C. Decarboxylative fluorination of aliphatic carboxylic acids via photoredox catalysis. J. Am. Chem. Soc. 2015, 137, 5654–5657. (b) Wu, X.; Meng, C.; Yuan, X.; Jia, X.; Qian, X.; Ye, J. Transition-metal-free visible-light photoredox catalysis at room temperature for decarboxylative fluorination of aliphatic carboxylic acids by organic dyes. Chem. Commun. 2015, 51, 11864–11867. (c) Wang, Z.; Guo, C.-Y.; Yang, C.; Chen, J.-P. Ag-catalyzed chemoselective decarboxylative monoand gem-difluorination of malonic acid derivatives. J. Am. Chem. Soc. 2019, 141, 5617–5622.
- (15) (a) Sladojevich, F.; Arlow, S. I.; Tang, P.; Ritter, T. Late-stage deoxyfluorination of alcohols with phenofluor. J. Am. Chem. Soc. 2013, 135, 2470–2473. (b) McTeague, T. A.; Jamison, T. F. Photoredox activation of SF6 for fluorination. Angew. Chem., Int. Ed. 2016, 55, 15072–15075. (c) Li, L.; Ni, C.; Wang, F.; Hu, J. Deoxyfluorination of alcohols with 3,3-difluoro-1,2-diarylcyclopropenes. Nat. Commun. 2016, 7, 13320. (d) Nielsen, M. K.; Ahneman, D. T.; Riera, O.; Doyle, A. G. Deoxyfluorination with sulfonyl fluorides: navigating reaction space with machine learning. J. Am. Chem. Soc. 2018, 140, 5004–5008.
- (16) (a) Rueda-Becerril, M.; Sazepin, C. C.; Leung, J. C. T.; Okbinoglu, T.; Kennepohl, P.; Paquin, J.-F.; Sammis, G. M. Fluorine transfer to alkyl radicals. *J. Am. Chem. Soc.* **2012**, *134*, 4026–4029. (b) Dang, H.; Mailig, M.; Lalic, G. Mild copper-catalyzed fluorination of alkyl triflates with potassium fluoride. *Angew. Chem., Int. Ed.* **2014**, 53, 6473–6476. (c) González-Esguevillas, M.; Miró, J.; Jeffrey, J. L.;

- MacMillan, D. W. C. Photoredox-catalyzed deoxyfluorination of activated alcohols with selectfluor. Tetrahedron 2019, 75, 4222-4227. (17) (a) Emer, E.; Pfeifer, L.; Brown, J. M.; Gouverneur, V. cis-Specific hydrofluorination of alkenylarenes under palladium catalysis through an ionic pathway. Angew. Chem., Int. Ed. 2014, 53, 4181-4185. (b) Lu, Z.; Zeng, X.; Hammond, G. B.; Xu, B. Widely applicable hydrofluorination of alkenes via bifunctional activation of hydrogen fluoride. J. Am. Chem. Soc. 2017, 139, 18202-18205. (c) Xie, Y.; Sun, P.-W.; Li, Y.; Wang, S.; Ye, M.; Li, Z. Ligand-promoted Iron(III)catalyzed hydrofluorination of alkenes. Angew. Chem., Int. Ed. 2019, 58, 7097-7101. (d) Braun, M.-G.; Katcher, M. H.; Doyle, A. G. Carbofluorination via a palladium-catalyzed cascade reaction. Chem. Sci. 2013, 4, 1216-1220. (e) Kindt, S.; Heinrich, M. R. Intermolecular radical carbofluorination of non-activated alkenes. Chem. - Eur. J. 2014, 20, 15344-15348. (f) Yuan, W.; Szabó, K. J. Catalytic intramolecular aminofluorination, oxyfluorination, and carbofluorination with a stable and versatile hypervalent fluoroiodine reagent. Angew. Chem., Int. Ed. 2015, 54, 8533-8537. (g) Liu, Z.; Chen, H.; Lv, Y.; Tan, X.; Shen, H.; Yu, H.-Z.; Li, C. Radical carbofluorination of unactivated alkenes with fluoride ions. J. Am. Chem. Soc. 2018, 140, 6169-6175. (h) Sorlin, A. M.; Mixdorf, J. C.; Rotella, M.; Martin, R.; Gutierrez, O.; Nguyen, H. M. The role of trichloroacetimidate to enable iridium-catalyzed regio- and enantioselective allylic fluorination: a combined experimental and computational study. J. Am. Chem. Soc. 2019, 141, 14843-14852.
- (18) (a) Jiang, X.; Sakthivel, S.; Kulbitski, K.; Nisnevich, G.; Gandelman, M. Efficient synthesis of secondary alkyl fluorides via Suzuki cross-coupling reaction of 1-halo-1-fluoroalkanes. *J. Am. Chem. Soc.* **2014**, *136*, 9548–9551. (b) Merchant, R. R.; Edwards, J. T.; Qin, T.; Kruszyk, M. M.; Bi, C.; Che, G.; Bao, D.-H.; Qiao, W.; Sun, L.; Collins, M. R.; Fadeyi, O. O.; Gallego, G. M.; Mousseau, J. J.; Nuhant, P.; Baran, P. S. Modular radical cross-coupling with sulfones enables access to sp³-rich (fluoro)alkylated scaffolds. *Science* **2018**, *360*, 75–80.
- (19) Sheng, J.; Ni, H.-Q.; Zhang, H.-R.; Zhang, K.-F.; Wang, Y.-N.; Wang, X.-S. Nickel-catalyzed reductive cross-coupling of aryl halides with monofluoroalkyl halides for late-stage monofluoroalkylation. *Angew. Chem., Int. Ed.* **2018**, *57*, 7634–7639.
- (20) (a) Liu, J.; Yuan, Q.; Toste, F. D.; Sigman, M. S. Enantioselective construction of remote tertiary carbon-fluorine bonds. *Nat. Chem.* **2019**, *11*, 710–715. (b) Sim, J.; Campbell, M. W.; Molander, G. A. Synthesis of α -fluoro- α -amino acid derivatives via photoredox catalyzed carbofluorination. *ACS Catal.* **2019**, *9*, 1558–1563.
- (21) Tanasova, M.; Yang, Q.; Olmsted, C. C.; Vasileiou, C.; Li, X.; Anyika, M.; Borhan, B. An unusual conformation of α -haloamides due to cooperative binding with zincated porphyrins. *Eur. J. Org. Chem.* **2009**, 2009, 4242–4253.
- (22) Zhang, F.; Song, J. Z. A novel general method for preparation of α -fluoro- α -arylcarboxylic acid. Direct fluorination of silylketene acetals with selectfluor. *Tetrahedron Lett.* **2006**, *47*, 7641–7644.
- (23) Laurent, S. A.-L.; Boissier, J.; Coslédan, F.; Gornitzka, H.; Robert, A.; Meunier, B. Synthesis of "Trioxaquantel" dericatives as potential new antischistosomal drugs. *Eur. J. Org. Chem.* **2008**, 2008 (5), 895–913.
- (24) Decarboxylative cross-coupling transformations involving carboxylic acids and their α -heteroatom variants under photoredox/Ni dual catalysis have been reported, but none of these focus on the use of α -fluoro acid substrates. For references, see: (a) Zuo, Z.; Ahneman, D. T.; Chu, L.; Terrett, J. A.; Doyle, A. G.; MacMillan, D. W. C. Dual catalysis. Merging photoredox with nickel catalysis: coupling of α -carboxyl sp³-carbons with aryl halides. *Science* **2014**, 345, 437–440. (b) Noble, A.; McCarver, S. J.; MacMillan, D. W. C. Merging photoredox and nickel catalysis: decarboxylative cross-coupling of carboxylic acids with vinyl halides. *J. Am. Chem. Soc.* **2015**, 137, 624–627. (c) Johnston, C. P.; Smith, R. T.; Allmendinger, S.; MacMillan, D. W. C. Metallaphotoredox-catalyzed sp³-sp³ cross-coupling of carboxylic acids with alkyl halides. *Nature* **2016**, 536, 322–325.

(25) Zhang, R.; Li, G.; Wismer, M.; Vachal, P.; Colletti, S. L.; Shi, Z.-C. Profiling and application of photoreodx C(sp³)-C(sp³) cross-coupling in medicinal chemistry. *ACS Med. Chem. Lett.* **2018**, *9*, 773–777.

(26) Specifically, optimizations were performed with unrestricted DFT (with guess = mix keyword) using DMA as model solvent and CPCM as implicit solvation model with Grimme's dispersion correction with original D3 damping [noted as UB3LYP-D3/def2-SVP-CPCM(DMA)] as implemented in Gaussian 09 (see Supporting Information for complete reference). Single-point energy calculations were then calculated using a larger basis set to provide more reliable energy values [noted as UB3LYP-D3/def2-TZVPP-CPCM(DMA)// UB3LYP-D3/def2-SVP-CPCM(DMA)]]. These methods have been applied extensively to investigate and predict reactivity and selectivity in transition metal-catalyzed transformations, including Ni-catalyzed cross-couplings. For simplicity, only the free energy values obtained from single-point energy calculations will be discussed in the manuscript (for other energetics, see Supporting Information). (a) Barone, V.; Cossi, M. Quantum calculation of molecular energies and energy gradients in solution by a conductor solvent model. J. Phys. Chem. A 1998, 102, 1995-2001. (b) Cossi, M.; Rega, N.; Scalmani, G.; Barone, V. Energies, structures, and electronic properties of molecules in solution with the C-PCM solvation model. J. Comput. Chem. 2003, 24, 669-681. (c) Grimme, S.; Antony, J.; Ehrlich, S.; Krieg, H. A consistent and accurate ab initio parameterization of density functional dispersion correction (DFT-D) for the 94 elements H-Pu. J. Chem. Phys. 2010, 132, 154104. For selected examples on computational analysis of nickel-catalyzed reactions, see: (d) Oshita, H.; Suzuki, T.; Kawashima, K.; Abe, H.; Tani, F.; Mori, S.; Yajima, T.; Shimazaki, Y. The effect of $\pi-\pi$ stacking interaction of the indole ring with the coordinated phenoxyl radical in a nickel(II)-salen type complex. Comparison with the corresponding Cu(II) complex. Dalton Trans 2019, 48, 12060-12069. (e) Slater, J. W.; Marguet, S. C.; Cirino, S. L.; Maugeri, P. T.; Shafaat, H. S. Experimental and DFT Investigations Reveal the Influence of the Outer Coordination Sphere on the Vibrational Spectra of Nickel- Substituted Rubredoxin, a Model Hydrogenase Enzyme. Inorg. Chem. 2017, 56, 3926-3938. (f) Matsui, J. K.; Gutierrez-Bonet, A.; Rotella, M.; Alam, R.; Gutierrez, O.; Molander, G. A. Photoredox/Nickel-Catalyzed Single-Electron Tsuji-Trost Reaction: Development and Mechanistic Insights. Angew. Chem. 2018, 130, 16073-16077. (g) Dohm, S.; Hansen, A.; Steinmetz, M.; Grimme, S.; Checinski, M. P. Comprehensive Thermochemical Benchmark Set of Realistic Closed-Shell Metal Organic Reactions. J. Chem. Theory Comput. 2018, 14, 2596-2608. (h) Yin, H.; Fu, G. C. Mechanistic Investigation of Enantioconvergent Kumada Reactions of Racemic α -Bromoketones Catalyzed by a Nickel/Bix(oxazoline) Complex. J. Am. Chem. Soc. 2019, 141, 15433-15440.

(27) (a) Yuan, M.; Song, Z.; Badir, S. O.; Molander, G. A.; Gutierrez, O. On The Nature of C(sp3)-C(sp2) Bond Formation in Nickel-Catalyzed Tertiary Radical Cross-Couplings: A Case Study of Ni/Photoredox Catalytic Cross-Coupling of Alkyl Radicals and Aryl Halides. J. Am. Chem. Soc. 2020, DOI: 10.1021/jacs.0c02355 (b) Luo, Y.; Gutierrez-Bonet, A.; Matsui, J. K.; Rotella, M. E.; Dykstra, R.; Gutierrez, O.; Molander, G. A. Oxa- and Azabenzonorbornadienes as Electrophilic Partners under Photoredox/Nickel Dual Catalysis. ACS Catal. 2019, 9, 8835-8842. (c) Desrosiers, J. N.; Wei, X.; Gutierrez, O.; Savoie, J.; Qu, B.; Zeng, X.; Lee, H.; Grinberg, N.; Haddad, N.; Yee, N. K.; Roschangar, F.; Song, J. J.; Kozlowski, M. C.; Senanayake, C. H. Nickel-catalyzed C-3 direct arylation of pyridinium ions for the synthesis of 1-azafluorenes. Chem. Sci. 2016, 7, 5581-5586. (d) Matsui, J.; Gutierrez-Bonet, A.; Rotella, M.; Alam, R.; Gutierrez, O.; Molander, G. A. Photoredox/Nickel-Catalyzed Single-Electron Tsuji-Trost Reaction: Development and Mechanistic Insight. Angew. Chem., Int. Ed. 2018, 57, 15847-15851. (e) Gutierrez, O.; Tellis, J. C.; Primer, D. N.; Molander, G. A.; Kozlowski, M. C. Nickel-Catalyzed Cross-Coupling of Photoredox Generated Radicals: Uncovering a General Manifold for Stereoconvergence in Nickel-Catalyzed Cross-Couplings. J. Am. Chem. Soc. 2015, 137, 4896-4899.

(28) We explored the Ni(0)/Ni(II) pathway and located a nucleophilic substitution transition state from Ni(0) leading to the generation of $[Ni(II)(Ar)]^+Br^-$ species as confirmed by intrinsic reaction coordinate (IRC) calculation, where Br was stabilized by aryl ring (see Figure S1 in Supporting Information for details). Contrarily, the concerted oxidative addition transition states were obtained with phenyl bromide and 4-methoxy-aryl bromide, leading to the generation of Ni(II) complex. Taken together, we attribute such difference in oxidative addition pathway to the electronic character of aryl ring (see Figure S5 for details).

(29) Although this step is slightly endergonic, analysis of the free energy span reveals that the low barrier of oxidative addition and the barrierless radical addition of benzyl radical on Ni(0) can drive the reaction forward and facilitate the turnover of catalytic cycle (see Figure S6 in Supporting Information for full details and associated discussion).

(30) Alternatively, the nature of a C–F bond versus a C–H bond leads to less electron density at the benzylic carbon and thus weakens the Ni–C(benzyl) interaction, as evident by a longer distance in ²E-P_B-TS-F vs ²E-P_B-TS-H, 2.22 vs 2.17 Å, respectively. We also observed similar trends using more electron-rich bipyrine ligands (See Supporting Information for energetics).

(31) (a) Wang, X.; Wang, S.; Xue, W.; Gong, H. Nickel-Catalyzed Reductive Coupling of Aryl Bromides with Tertiary Alkyl Halides. *J. Am. Chem. Soc.* **2015**, *137*, 11562–11565. (b) Primer, D. N.; Molander, G. A. Enabling the Cross-Coupling of Tertiary Organoboron Nucleophiles through Radical-Mediated Alkyl Transfer. *J. Am. Chem. Soc.* **2017**, *139*, 9847–9850.

(32) On the basis of the calculated results with both L1 (see Figure S3 in the Supporting Information) and L2 (t-Bu groups were truncated as Me groups, see Figure S1 in the Supporting Information), we observed that the barrier of Ni(I)/Ni(III) oxidative addition is lower (12.6 kcal/mol via ²B-C-TS-OMe-F) using more electron-rich L1 than using less-electron rich L2 (13.6 via ²B-C-TS-F). Moreover, we found that the relative barriers for reductive elimination with L1 (between ²E-P_B-TS-OMe-F and ¹D-OMe) and that with L2 (between ²E-P_B-TS-F and ¹D) are similar (13.5 vs 13.7 kcal/mol)). On the basis of these observations, the diminished yield observed for more electron-deficient L2 and L3 (in comparison to L1) could be due to higher barriers for the oxidative addition step in the Ni(I)/Ni(III) pathway. More importantly, comparing the barrier of Ni(I)/Ni(III) oxidative addition and reductive elimination, for the L1 system the barrier of reductive elimination is higher by 1.1 kcal/ mol; thus, the reductive elimination step should be more rate-limiting than the Ni(I)/Ni(III) oxidative addition step in this case. However, for the L2 system, the difference in the barrier of these two steps is very small (only 0.2 kcal/mol); thus, the Ni(I)/Ni(III) oxidative addition step might also limit the reaction rate in this case. Taken together, the promoted barrier of Ni(I)/Ni(III) oxidative addition could explain the decreased reaction yield when switching to the more electron-deficient ligand.

(33) (a) Heitz, D. R.; Tellis, J. C.; Molander, G. A. Photochemical Nickel-catalyzed C-H arylation: synthetic scope and mechanistic investigations. *J. Am. Chem. Soc.* **2016**, *138*, 12715–12718. (b) Paul, S.; Guin, J. Radical C(sp³)-H alkenylation, alkynylation and allylation of ethers and amides enabled by photocatalysis. *Green Chem.* **2017**, *19*, 2530–2534.

(34) (a) Lovinger, G. J.; Aparece, M. D.; Morken, J. P. Pd-catalyzed conjunctive cross-coupling between Grignard-derived boron "ate" complexes and C(sp²) halides or triflates: NaOTf as a Grignard activator and halide scavenger. *J. Am. Chem. Soc.* **2017**, *139*, 3153–3160. (b) Ackerman, L. K. G.; Lovell, M. M.; Weix, D. J. Multimetallic catalyzed cross-coupling of aryl bromides with aryl triflates. *Nature* **2015**, *524*, 454–457.

(35) We detected small and varying amounts of the hydrodefluorinated derivative of 1a in some cases during our optimization studies in Table 1, suggesting the formation of fluoride in the system. In addition, performing the model reaction under standard conditions (Table 1, entry 1) using KF (1 equiv.) instead of KOTf as the additive

completely suppressed the reaction (<2% conv.). For a representative example of fluoride inhibition on nickel catalysis, see: Colon, I.; Kelsey, D. R. Coupling of Aryl Chlorides by Nickel and Reducing Metals. *J. Org. Chem.* **1986**, *51*, 2627–2637.

- (36) (a) Sun, D.; Wang, Z.; Cardozo, M.; Choi, R.; Degraffenreid, M.; Di, Y.; He, X.; Jaen, J. c.; Labelle, M.; Liu, J.; Ma, J.; Miao, S.; Sudom, A.; Tang, L.; Tu, H.; Ursu, S.; Walker, N.; Yan, X.; Ye, Q.; Powers, J. P. Synthesis and optimization of arylsulfonylpiperazines as a novel class of inhibitors of 11β -hydroxysteroid dehydrogenase type 1 (11β -HSD1). Bioorg. Med. Chem. Lett. **2009**, 19, 1522–1527. (b) Buckley, D. I.; Duke, G.; Wagman, A. S.; Evanchik, M.; McDowell, R. S. Heterocyclic modulators of lipid synthesis. U.S. Patent No. WO 2018/089904, May 17, 2018.
- (37) Purohit, A.; Benetti, R.; Hayes, M.; Guaraldi, M.; Kagan, M.; Yalamanchilli, P.; Su, F.; Azure, M.; Mistry, M.; Yu, M.; Robinson, S.; Dischino, D. D.; Casebier, D. Quinazoline derivatives as MC-I inhibitors: evaluation of myocardial uptake using positron emission tomography in rat and non-human primate. *Bioorg. Med. Chem. Lett.* **2007**, *17*, 4882–4885.
- (38) Koperniku, A.; Liu, H.; Hurley, P. B. Mono- and difluorination of benzylic carbon atoms. *Eur. J. Org. Chem.* **2016**, 2016, 871–886. (39) Hu, W.-L.; Hu, X.-G.; Hunter, L. Recent developments in the
- (39) Hu, W.-L.; Hu, X.-G.; Hunter, L. Recent developments in the deoxyfluorination of alcohols and phenols: new reagents, mechanistic insights, and applications. *Synthesis* **2017**, *49*, 4917–4930.